Proc. Annual Meeting of the Austrian Society for Biomedical Engineering 2021
DOI: 10.3217/978-3-85125-826-4-21

AN INVESTIGATION ON DIMENSIONALITY REDUCTION IN THE SOURCE-SPACE-BASED HAND TRAJECTORY DECODING

Nitikorn Srisrisawang[1], Gernot Müller-Putz[1]

[1] Institute of Neural Engineering, Graz University of Technology, Graz, Austria

E-mail: gernot.mueller@tugraz.at

Abstract— *In this work, the hand trajectory decoding was investigated in the source space. A couple of dimensionality reduction techniques were utilized to reduce the number of the source-space signals, namely, computing the mean, principle component analysis (PCA), locality preserving projection (LPP).*
The decoding performances from the source-space approaches were compared to the sensor-space approach. We found that every approach showed performance metrics in a similar range and only slight differences across approaches could be observed. The source-space approach with PCA with 8 components exhibited higher performance metrics than other approaches and slightly higher performance metrics than the sensor-space approach (improvement for correlation 0.01 to 0.09, SNR 0.05 to 0.1 dB). The results suggested that the source-space-based decoding is possible, and it can achieve comparable performance to the sensor-space approach.

Keywords— *EEG, BCI, source localization, PCA, LPP, PLS, UKF, hand trajectory decoding*

Introduction

The electroencephalogram (EEG) measures the electrical changes of the brain non-invasively. Since the actual underlying sources in the brain are inaccessible from EEG, source localization is utilized to estimate the underlying cortical sources. The source localization is rarely implemented in the processing steps but rather in the post-analysis because of the complexity of the problem.
Recently, some studies investigated this direction. They demonstrated the possibility of source-space classification in brain-computer interfacing (BCI) [1]–[4]. Still, only single literature [5] focused on the regression problem, so this work will explore the possibility of regression of hand trajectory in the source space.

Previously, a couple of works from our group [6]–[9] studied the decoding of hand movement trajectory for the pursuit tracking task (PTT) from EEG in an online setting. Group-level source localization analysis reveals the brain regions contributing to the decoding of the movement kinematics to be located between the medial part of the frontal and parietal area, which corresponds to the frontoparietal network [10]. This information could be used to restrict the signals in the source space, but the resulting number of signals is still in the range of thousands. Hence, different dimensionality reduction techniques widely used in different research fields were investigated, namely, principal component analysis (PCA), locality preserving projection (LPP) [11], and computing the mean.

Methods

Dataset description

The data from 2 studies [8], [9] was used. In total, there are 15 measurements from 14 different participants since one participant was in both studies while one participant was excluded due to the signal quality in some measurement runs.

Experimental setup

The task for the participant was to follow a target cursor ("snake") on the screen by controlling a robotic arm (JACO, Kinova Robotics Inc., Canada) via a mixed control between the hand movement, captured via the LeapMotion (LM) system (LeapMotion Inc., USA), and the decoded signal from EEG. The mixed percentage of the control was adjusted to the respective run from 100% LM and 0% EEG to 0% LM and 100% EEG. The EEG signals were simultaneously measured via 64 (in [8]) and 60 (in [9]) active EEG electrodes (actiCAP, Brain Products GmbH., Germany) recorded at 500 Hz with biosignal amplifiers (BrainAmp, Brain Products GmbH, Germany). The common EEG channels between both studies used in this analysis can be seen

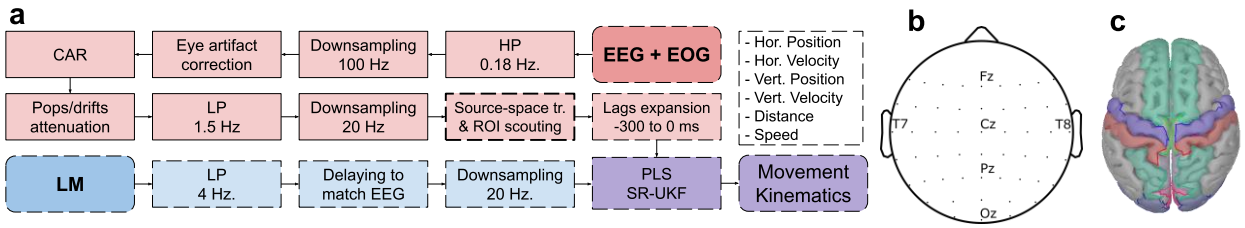

Figure 1: Overview of the experiment information a) common processing pipeline adapted from [7], [8] with additional source-space transformation and ROI scouting block, highlighted with dashed lines, b) common electrodes position used in the analysis, c) the predefined region-of-interest

Published by Verlag der TU Graz
Graz University of Technology

DOI: 10.3217/978-3-85125-826-4-21

in Fig. 1b. The data from the 100% LM was used to calibrate the decoding model. For a detailed explanation of the experimental setup, please refer to [8], [9]

Processing Pipeline

The overview of the processing was shown in Fig.1a. For a detailed description of the processing pipeline, please refer to [8], [9], on which the processing pipeline was based. The following changes were made in the processing pipeline. 1. an additional source-space transformation and ROI scouting block were added 2. criteria for choosing the retained number of components in the partial least square (PLS) model were to retain 95% of total variances components instead of fixing the same number of components across measurements. The combination between PLS and the square roots unscented Kalman filter (SR-UKF) [12] produces the following movement kinematics: horizontal position, vertical position, horizontal velocity, vertical velocity, speed, and distance.

Source-space transformation

Before the experiment, electrode positions were measured. This information was used to co-register with an ICBM152 template head model. The forward problem was modeled with a boundary element method (BEM) with 5000 unconstrained cortical dipole sources, meaning that each source was modeled with 3 components in XYZ directions. The conductivity of the scalp, skull, and brain was set to (0.41, 0.02, 0.47) [13], respectively. The inverse problem was solved with OpenMEEG [14] and sLORETA [15] using the Brainstorm package [16].

ROI scouting

Several regions-of-interests (ROIs) were defined according to the Mindboggle brain atlas [17] to reduce the number of signals in the source space. The predefined ROIs, which were based on the frontoparietal network [6], [10], are as follows: cuneus, lateral occipital, paracentral, postcentral, precentral, precuneus, superior frontal, and superior parietal in both hemispheres (Fig. 1c). Different dimensionality reduction techniques were employed for each directional component of sources in each ROI to reduce the number of signals further. These are PCA, LPP [11], and computing the mean signals. The optimum number of retained components for both PCA and LPP were chosen by comparing the correlation and the computational complexity of 1,2,4,8, and 16 components. For both PCA and LPP, 8 components were retained per each directional source component or equivalently 24 components per ROI. The processes of source-space transformation and ROI scouting can be summarized as matrix multiplications as:

$$\mathrm{Y} = SKX \tag{1}$$

where X is processed sensor-space EEG signals, K is a kernel matrix that transforms sensor-space signals into the source space, S is a scouting matrix that produces the representation signals Y from the source-space signals.

Decoding performance evaluation

The following metrics were chosen to compare among the different approaches. Namely, the correlation between the decoded and the actual trajectory, signal-to-noise (SNR) ratio defined as:

$$\mathrm{SNR}(\mathrm{z_t}, \widehat{z_t}) = 10 \log_{10} \frac{\mathrm{var}(\mathrm{z_t})}{mse(\mathrm{z_t}, \widehat{z_t})} \tag{2}$$

and decoded-signals-to-signal (DSSR) ratio defined as [7]:

$$\mathrm{DSSR}(\mathrm{z_t}, \widehat{z_t}) = 10 \log_{10} \frac{\mathrm{var}(\mathrm{z_t})}{\mathrm{var}(\widehat{z_t})} \tag{3}$$

where $\mathrm{z_t}, \widehat{z_t}$ indicate the true and the decoded kinematics, $\mathrm{var}(x)$ means the variance of x and $mse(x, y)$ means the mean squared error (MSE) between x and y. The DSSR [7] could be interpreted as the amplitude mismatch between the decoded and the actual movement kinematics. The best case is that the amplitude of kinematics matches with a DSSR at 0 dB. The horizontal and vertical components were grouped by computing the mean and distance and speed into position, velocity, and magnitude. The 3 kinematics will be called 'simplified' kinematics, and they were meant only for visualization purposes, while the 'full' kinematics contain the original 6 kinematics. The metrics differences between 'Se' and the best source-space approach for each of the 'full' kinematics were computed by subtracting the best source-space approach to 'Se' from the same measurement and then computing the mean across measurements.

Statistical evaluation

The experiment was repeated in a simulated manner that closely resembles the online processing pipeline with different approaches: sensor-based approach *'Se'*, computing the mean *'Mean'*, *'PCA8'*, and *'LPP8'*. The subject-level average metrics were computed. Multiway repeated-measures ANOVA was used to compare the following factors: 1. control percentage (100% LM – 0% LM), 2. movement kinematics, and 3. different approaches ('Se', 'Mean', 'PCA8', 'LPP8'), using Greenhouse-Geisser correction. For the DSSR, the absolute value was used in the statistical test (aDSSR). Tukey's HSD test was used as a post-hoc test for multiple comparisons. These statistical tests were performed on the 'full' kinematics.

Results

The results from the 'simplified' kinematics were summarized in Fig. 2. Overall, the boxplots revealed the trends where the directional kinematics indicated higher performance than the non-directional ones.
From Fig. 2., every approach showed the median correlations in a similar range at around 0.30, 0.32, 0.12

Published by Verlag der TU Graz
Graz University of Technology

DOI: 10.3217/978-3-85125-826-4-21

for the position, velocity, and magnitude. 'PCA8' exhibited a higher median correlation in velocity and magnitude than 'Se'.

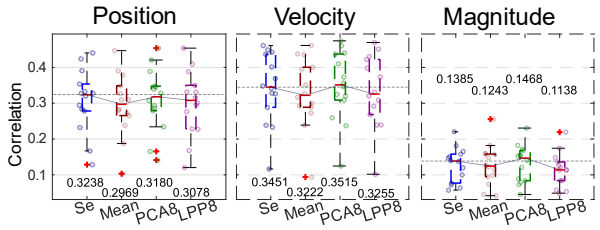

Figure 2: The subject-level boxplot correlation of different approaches, *'Se', 'Mean', 'PCA8', 'LPP8'*. For visualization purposes, the 'simplified' kinematics were used, and the mean of the correlations was computed across 100%LM to 0%LM runs. The numbers indicate the corresponding median values. The dashed lines indicate the median value of 'Se'.

Multiway repeated-measures ANOVA revealed statistically significant differences between approaches in terms of correlation ($F(3,39)=5.5$, $p=0.010$), SNR ($F(3,39)=5.1$, $p=4.15\times10^{-5}$), but not in the case of absolute DSSR ($F(3,39)=2.47$, $p=0.101$).
Post-hoc tests revealed that 'Mean' and 'LPP8' showed lower performance than 'Se' and that 'PCA8' indicated slightly higher performance than the rest. The only statistically significant results were between a pair of 'LPP8' to 'PCA8' ($p=0.018$), while the other comparison between pairs was not statistically significant. The performance's ranking is as follows: 'PCA8' > 'Se' > 'Mean' > 'LPP8'. The group-level differences between 'PCA8' and 'Se' of the 'full' kinematics can be found in Tab. 1. In most cases for correlation and SNR, 'PCA8' showed slightly higher performance than 'Se'.

Table 1: Group-level differences of 'PCA8' and 'Se' from 'full' kinematics

	Corr.	**SNR**	**aDSSR**
Pos. X	0.0009	0.1084	-0.0121
Vel. X	0.0049	-0.0165	-0.04
Pos. Y	0.0035	0.0938	-0.0454
Vel. Y	0.0084	-0.02	-0.0588
Distance	-0.0015	0.0704	0.0282
Speed	0.0096	0.0499	0.0503

Discussion

Several works had proven that the decoding of hand movement trajectory in humans based on the sensor-space EEG signals could be done with an actual hand movement [8], [9], or imagined hand movement [18]. However, an open question was whether it is possible to perform decoding of hand movement trajectory based on the source-space signals.
To answer that, we tried several approaches to overcome the problem of a high number of signals in the source space, namely, 'Mean', 'PCA8', 'LPP8'.
The processing pipeline of 'Se' is the same as in [9], and the results indicated the correlations of 'Se' to be in a similar range. Comparing 'Se' to the source space approaches ('Mean', 'PCA8', 'LPP8'), we see the performance in a similar range as in 'Se' with some slight differences. It is indicated via post-hoc tests that among all approaches, 'PCA8' could perform slightly better than 'Se', but the differences were not statistically significant. The results showed that the decoding in the source space is possible with comparable performance, and the best candidate out of all could be 'PCA8'.
We have the following assumptions to explain the cause of the lower performance of 'Mean'. First, the number of signals from 'Mean' was reduced from each ROI with the original number of signals in a range between hundreds to thousands of signals per ROI, to just 3 signals (1 for each direction of the source components), and this could retain very little information. Second, by using the mean function, we assumed the distribution of the signals in each ROI to be normally distributed, which was hardly the case in this situation. In LPP, it was introduced as a dimensionality reduction technique that tries to retain the local network structure in the lower dimension [11]. This technique was successfully applied in the computer vision field and the BCI field [19]. However, the results suggested the performance of LPP to be the worse among the candidates. The worse performance could be due to the difference between classification problems (as LPP was typically used) and the regression.
Some works [1]–[4] that utilized the source-space information in the classification problem indicated some improvement over the sensor space. However, Sosnik and Zheng 2021 [5], who investigated the decoding of joints kinematics with signals in the source space, showed slightly lower performance than the sensor space. Their approach was comparable with our 'Mean' approach, which also showed slightly lower performance than 'Se'.
There are some interesting points to further explore for the source-space-based decoding: the benefits of incorporating the individualized anatomical information from the magnetic resonance imaging (MRI) and how the decoding behaves in the actual online experiment.

Conclusion

Different reduction techniques were implemented to overcome the problem of a high number of signals. By comparing the performance metrics from the sensor-space approach, 'Se', to the source-space approaches, 'Mean', 'PCA8', 'LPP8', we found that only the 'PCA8' could perform better than 'Se'. However, the differences were only marginal and not statistically significant. The results suggested that the source-space-based decoding of hand movement trajectory is possible with comparable performance to 'Se'.

Published by Verlag der TU Graz
Graz University of Technology

DOI: 10.3217/978-3-85125-826-4-21

Acknowledgements

Research supported by funding from the European Research Council (ERC-CoG-2015 681231 'Feel Your Reach'), the author N.S. received funding from the Royal Thai Government.

References

[1] L. Qin, L. Ding, and B. He, “Motor imagery classification by means of source analysis for brain–computer interface applications,” *J. Neural Eng.*, vol. 1, no. 3, pp. 135–141, Sep. 2004, doi: 10.1088/1741-2560/1/3/002.

[2] B. J. Edelman *et al.*, “Noninvasive neuroimaging enhances continuous neural tracking for robotic device control,” *Sci. Robot.*, vol. 4, no. 31, p. eaaw6844, Jun. 2019, doi: 10.1126/scirobotics.aaw6844.

[3] C. Li, H. Guan, Z. Huang, W. Chen, J. Li, and S. Zhang, “Improving Movement-Related Cortical Potential Detection at the EEG Source Domain,” in *2021 10th International IEEE/EMBS Conference on Neural Engineering (NER)*, Italy, May 2021, pp. 214–217. doi: 10.1109/NER49283.2021.9441169.

[4] V. Shenoy Handiru, A. P. Vinod, and C. Guan, “EEG source space analysis of the supervised factor analytic approach for the classification of multi-directional arm movement,” *J. Neural Eng.*, vol. 14, no. 4, p. 046008, Aug. 2017, doi: 10.1088/1741-2552/aa6baf.

[5] R. Sosnik and L. Zheng, “Reconstruction of hand, elbow and shoulder actual and imagined trajectories in 3D space using EEG current source dipoles,” *J. Neural Eng.*, vol. 18, no. 5, p. 056011, Oct. 2021, doi: 10.1088/1741-2552/abf0d7.

[6] R. J. Kobler, A. I. Sburlea, and G. R. Müller-Putz, “Tuning characteristics of low-frequency EEG to positions and velocities in visuomotor and oculomotor tracking tasks,” *Sci. Rep.*, vol. 8, no. 1, p. 17713, Dec. 2018, doi: 10.1038/s41598-018-36326-y.

[7] R. J. Kobler, A. I. Sburlea, V. Mondini, M. Hirata, and G. R. Müller-Putz, “Distance- and speed-informed kinematics decoding improves M/EEG based upper-limb movement decoder accuracy,” *J. Neural Eng.*, Aug. 2020, doi: 10.1088/1741-2552/abb3b3.

[8] V. Mondini, R. J. Kobler, A. I. Sburlea, and G. R. Müller-Putz, “Continuous low-frequency EEG decoding of arm movement for closed-loop, natural control of a robotic arm,” *J. Neural Eng.*, Jul. 2020, doi: 10.1088/1741-2552/aba6f7.

[9] V. Martınez-Cagigal, R. J. Kobler, V. Mondini, R. Hornero, and G. R. Muller-Putz, “Non-Linear Online Low-Frequency EEG Decoding of Arm Movements During a Pursuit Tracking Task,” *2020 42nd Annu. Int. Conf. IEEE Eng. Med. Biol. Soc. EMBC*, p. 5, doi: 10.1109/EMBC44109.2020.9175723.

[10] J. C. Culham and K. F. Valyear, “Human parietal cortex in action,” *Curr. Opin. Neurobiol.*, vol. 16, no. 2, pp. 205–212, Apr. 2006, doi: 10.1016/j.conb.2006.03.005.

[11] X. He and P. Niyogi, “Locality Preserving Projections,” in *Advances in Neural Information Processing Systems 16*, 2004, p. 8.

[12] R. Van der Merwe and E. A. Wan, “The square-root unscented Kalman filter for state and parameter-estimation,” in *2001 IEEE International Conference on Acoustics, Speech, and Signal Processing. Proceedings (Cat. No.01CH37221)*, Salt Lake City, UT, USA, 2001, vol. 6, pp. 3461–3464. doi: 10.1109/ICASSP.2001.940586.

[13] H. McCann, G. Pisano, and L. Beltrachini, “Variation in Reported Human Head Tissue Electrical Conductivity Values,” *Brain Topogr.*, vol. 32, no. 5, pp. 825–858, Sep. 2019, doi: 10.1007/s10548-019-00710-2.

[14] A. Gramfort, T. Papadopoulo, E. Olivi, and M. Clerc, “OpenMEEG: opensource software for quasistatic bioelectromagnetics,” *Biomed. Eng. OnLine*, vol. 9, no. 1, p. 45, 2010, doi: 10.1186/1475-925X-9-45.

[15] R. D. Pascual-Marqui, “Standardized low-resolution brain electromagnetic tomography (sLORETA): technical details,” *Methods Find. Exp. Clin. Pharmacol.*, p. 16, 2002.

[16] F. Tadel, S. Baillet, J. C. Mosher, D. Pantazis, and R. M. Leahy, “Brainstorm: A User-Friendly Application for MEG/EEG Analysis,” *Comput. Intell. Neurosci.*, vol. 2011, pp. 1–13, 2011, doi: 10.1155/2011/879716.

[17] A. Klein *et al.*, “Mindboggling morphometry of human brains,” *PLOS Comput. Biol.*, vol. 13, no. 2, p. e1005350, Feb. 2017, doi: 10.1371/journal.pcbi.1005350.

[18] A. Korik, “Decoding Imagined 3D Hand Movement Trajectories From EEG: Evidence to Support the Use of Mu, Beta, and Low Gamma Oscillations,” *Front. Neurosci.*, vol. 12, p. 16, 2018, doi: 10.3389/fnins.2018.00130. PMID: 29615848.

[19] Ren Xu, Ning Jiang, Chuang Lin, N. Mrachacz-Kersting, K. Dremstrup, and D. Farina, “Enhanced Low-Latency Detection of Motor Intention From EEG for Closed-Loop Brain-Computer Interface Applications,” *IEEE Trans. Biomed. Eng.*, vol. 61, no. 2, pp. 288–296, Feb. 2014, doi: 10.1109/TBME.2013.2294203.

Published by Verlag der TU Graz
Graz University of Technology